Geomagnetic Disturbance accompanying the High Altitude Nuclear Deto-nation at Johnston Island on July 9th.1962

Geomagnetic Disturbance accompanying the High Altitude Nuclear Detonation at Johnston Island on July 9th, 1962

By Yoshio Kato and Shigeo Takei

Geophysical Institute, Faculty of Science, Tôhoku University

(Received March 20, 1963)

Abstract

In this paper the authors treat the propagation of the isotropic mode of the hydromagnetic waves in the magnetosphere and calculated the travel-time curve of that wave emitted from various sources and compared it with the time of commencement of the geomagnetic disturbance accompanying the high altitude nuclear detonation at Johnston Island on July 9th, 1962. Since the observed delay time was too short, the mechanism of magnetic transient variations produced by this high altitude nuclear detonation is not simple.

1 Introduction

A high altitude nuclear detonation was exploded in the vicinity of Johnston Island, 16.7N°–169.4°W, at $09^h00^m09^s$ U.T. on July 9th, 1962. Detonation height was reported to be about 400 km. Its effects on the earth's magnetic field were recorded at all magnetic observatories in the world.

In this paper we treated the propagation of the isotropic mode of the hydromagnetic waves in the magnetosphere assuming its various sources, and calculated the travel-time curves theoretically and compared them with the time of commencement of the geomagnetic disturbance because its first movement had been supposed as a hydromagnetic impulse. But the observed delay time was too short, therefore it appears that no simple explanation of the magnetic distrubance can be expected.

2 Alfvén wave velocity in the magnetosphere

The first impulse observed on the magnetogram is expected as the fast elementary hydromagnetic impulse, radiated from the source area. Therefore we can adopt the ray path theory only to discuss the distribution of the time of commencement of the magnetic impulse observed on the magnetogram. In this case we treated the propagation of the isotropic mode of the hydromagnetic wave.

To find the distribution of Alfvén velocity we constructed the model atmosphere above F2 region under the following assumptions;

1) The atmosphere has a spherically layered structure.
2) The isothermal diffusive equilibrium state.
3) The velocity distributions of ions and electrons are isotropic.
4) H^+, He^+, O^+ and electrons are considered as composition.
5) Electrical nutrality.

Under these assumptions we calculated the distribution of number densities of the ions above the reference level of 500 km. (Fig. 1) The initial values at this level are shown in Table I.

Below the reference level to 210 km, reference was made to the model adopted by H. Kamiyama which consisted of O^+, O_2^+ and nutral atoms and molecules.

Table I. Number densities of the ions at the reference level (after BATES & PATTERSON)

	H^+	He^+	O^+	Temperature
Number/cm³	1.8×10^2	4×10^3	4×10^5	1250°K

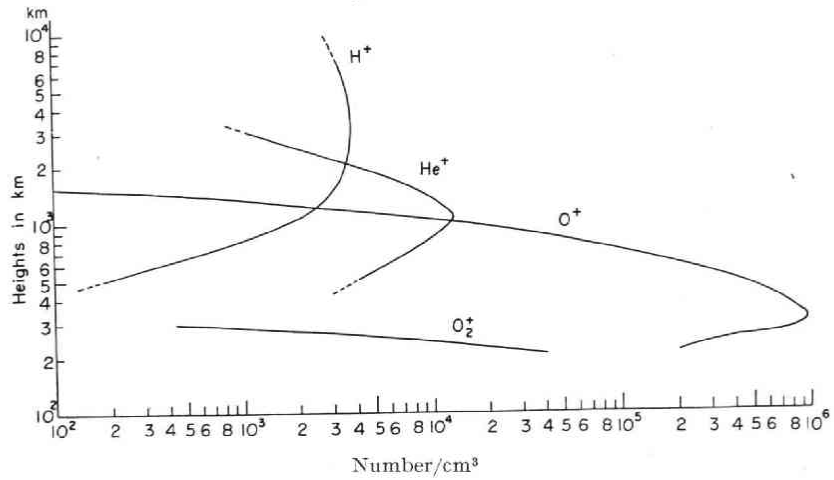

Fig. 1. Distribution of ions in the lower exosphere

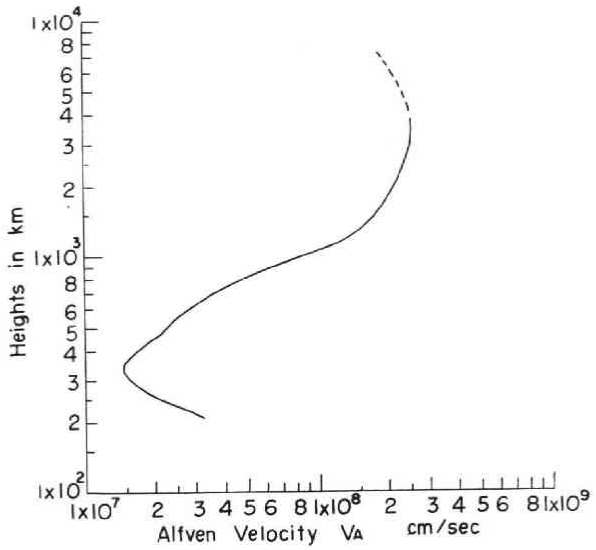

Fig. 2. Distribution of Alfvén Wave Velocity in the lower exosphere

Fig. 2 shows the calculated value of Alfvén wave velocity in the lower exosphere of the above stated composition after assuming that the magnetic field is the dipole magnetic field.

As the figure shows the maximum velocity, about 2500 km/sec, is held at the height of 3300 km and a low velocity layer is above the F2 peak.

3 The ray path and travel-time

The ray path which is supposed to represent the initial disturbance should be determined from the condition that the travel time T along the ray path is minimum.

Thus the travel-time $T\ [r]$, must be at the minimum in the propagation. (Fig. 3)

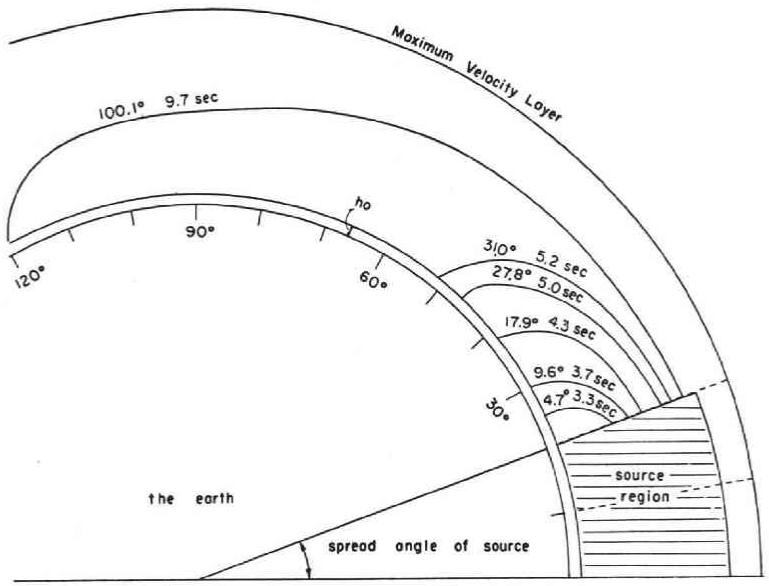

Fig. 3. Schematic showing of ray path geometry

$$T\left[r\left(\phi\right)\right] = \int \frac{ds}{V_A} = \int_{\phi_0}^{\phi_1} \frac{\sqrt{r^2 + r'^2}}{V(r)}\, d\phi = \int_{\phi_0}^{\phi_1} F\left(r \cdot r'\right) d\,\phi \tag{1}$$

where V_A is the velocity of ALFVÉN wave and is $\sqrt{B_0^2/4\pi\rho_0}$, and

$$r' = \frac{dr}{d\phi}$$

while

$$\delta T = \delta \int_{\phi_0}^{\phi_1} F\left(r,\, r'\right) \delta\, r\, d\,\phi = \int_{\phi_0}^{\phi_1} [F]_r\, \delta r d\phi + \left[F r'\, \delta r\right]_{\phi_0}^{\phi_1} = 0 \tag{2}$$

where $[F]_r$ is the first variation of T, and

$$Fr' = \frac{\partial F}{\partial r'}$$

The first term of equation (2) must vanish for the permitted paths. Therefore we can yield EULER's equation.

$$[F]_r = \frac{\partial F}{\partial r} - \frac{d}{d\phi}\left(\frac{\partial F}{\partial r'}\right) = 0$$

This equation is easily integrated when $\partial F/\partial\phi = 0$, that is;

$$F - r' Fr' = C \tag{3}$$

C is an integral constant and determines the behavior of the ray path. From equation (3)

$$\frac{dr}{d\phi} = \pm \frac{r\sqrt{r^2 - C^2V^2(r)}}{CV(r)} \tag{4}$$

Double sign in the equation (4) indicate that two symmetric paths for the source are permitted for the same value of C.

We take conveniently the plus sign for the expression of ray paths. Thus,

$$\phi = \int_{r(\phi_0)}^{r} \frac{CV(r)}{\sqrt{r^2 - C^2V^2}} \frac{dr}{r} \tag{5}$$

$$T = \int_{r(\phi_0)}^{r(\phi_1)} \frac{r\,dr}{V(r)\sqrt{r^2 - C^2V^2}} \tag{6}$$

It is mathematically clear that the actual paths are restricted within the region satisfying the condition

$$r^2 - C^2V^2(r) \geqq 0 \tag{7}$$

and the total reflection occurs if the equal sign is held, since such a point is the branch point of the ray paths.

To determine the parameter C, the boundary conditions at source area and the observation point is considered as follows.

$\delta r = 0$	at $\phi = \phi_1$ (observation point)	fixed condition
$\delta r \neq 0$	at $\phi = \phi_0$ (source area)	free condition

for $\underline{r}_0 < r < \bar{r}_0$, where $\underline{r}_0$ and $\bar{r}_0$ are the upper and lower bounds of the source

From the second term of the equation (2) we have

$$Fr' = \frac{Cr'}{r} = \frac{C}{r^2}\frac{dr}{d\phi} = 0 \qquad \text{at } \phi = \phi_0 \tag{8}$$

This implies that the fast path must start with the rectangular emergent angle. Connecting the equation (4) and (8), C is determined as follows;

$$C = \frac{r(\phi_0)}{V(r(\phi_0))} \tag{9}$$

But in the case of point source, C is not determined. In this case a path starting from the boundary of the source i.e. $r(\phi_0)=\bar{r}_0$ or $\underline{r}_0$, C is not restricted and is chosen freely. But since ϕ and T depends on C uniquely, the travel-time curve is determined uniquely for the given point $(r=r_1,\ \phi=\phi_1)$.

To calculate numerically, we adopted the following equation, equivalent to the equation (5), as it is known as SNELL's law in the polar coordinate.

$$\frac{r \sin i}{V} = C \tag{10}$$

where i is the incident angle, at first the paramenter C is determined by the equation (9) and the mesh of the integration was chosen as 1/500 earth radius.

4 Numerical results*

Fig. 4 shows the calculated travel-time cruve. In the figure the chain lines show the case of point source and full and dotted lines show the case of the sources

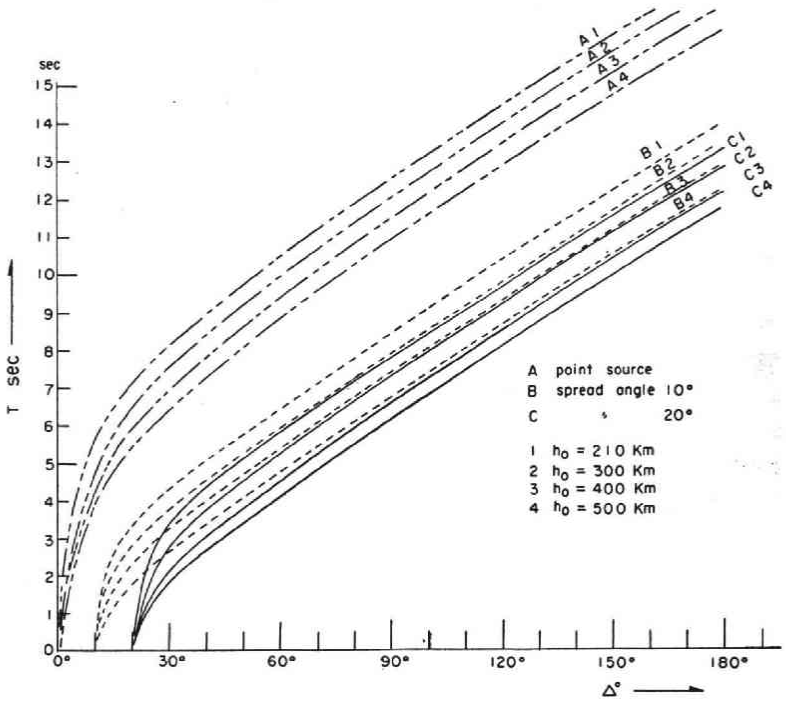

Fig. 4. Calculated travel-time curve:
the solid lines correspond to the source angle 20°
the dotted lines correspond to the source angle 10°
the chain corresponds to the case of point source

* These calculations were carried out by means of the electronic computer SENAC-1, of Computing Center, Tôhoku University.

whose spread angle of the source is 20° and 10° respectively, and nearly parallel curves in each case correspond to the assumed heights of the exospheric base which is taken to be 210 km, 300 km, 400 km and 500 km respectively and we assumed that the energy of the hydromagnetic wave is propagated electromagnetically below these heights.

As the figure shows, the difference between the case of point source and others is large. This depends on the boundary condition in each cases.

The effect of the difference in spread angles of the source appears in shifting the curve horizontally along with the coordinate of time T. While the effect of the difference in assumed base of the exosphere appears in shifting the curve nearly vertically along with the coordinate of distance.

5 Observed data and discussions

The initial movement on the normal run magnetogram due to the detonation is sufficiently large and observed at almost all the magnetic stations over the world but unfortunately it appears likely in the hour mark gap.

Furthermore because of the low chart speeds it was difficult to detect the accurate time of commencement.

But the specially provided magnetometer at the Victoria Magnetic Observatory recorded the commencement of the movement. B. CANER and K. WHITHAM reported and discussed the detonation effect on the geomagnetic field and concluded that the hydromagnetic wave propagated much faster than expected from the mean theoretical velocities and they suggested that it may not be reasonable to describe the propagated distrubance in terms of simple hydromagnetic waves.

Besides the Victoria data the La-Cour type magnetogram in the United States Zone and induction magnetogram in Japan or France and other countries are available to determine the commencement time of the movement although the accuracy of the timing is not so high.

SELZER reported the observational results of the detonation effect on the magnetic field and concluded that the microstructure of the perturbation looked about the same at the stations in France and he reported that the signal reached the whole world in less than a second and concluded that at least the front part of the signal may have a electromagnetic nature.

While Fig. 5 shows our calculated travel-time curve in case that the spread angle of source is 20°, and the base of the magnetosphere is 500 km or 400 km, comparing with the observed commencement time of distrubance at various stations in the world.

As the figure shows, the observed delay time is much shorter than the calculated value in the distant stations. Therefore it is suggested that the propagated disturbance is not explained in terms of simple hydromagnetic waves and it may be considered that the disturbance propagated electromagnetically in its most part of the path in or below the ionosphere. But the accuracy of the timing of the records is not sufficient to give a definite conclusion.

List of Stations

	Station	Distance	Travel Time (sec)
Ho	Honolulu	11°	− 0.1
Sh	Shimosato	43°	2.9
Gu	Guam	45°	2.5
Si	Sitka	48°	2.4
V	Victoria	50°	2.2
Co	College	51°	1.1
Cl	China Lake	55°	1.5±1.5
P	Point Barrow	56°	4.6
B	Brisbane	57°	1.0±1
Tu	Tucson	58°	2.9
A	Adélie	86°	3.0±1.5
F	Fredericksburg	91°	2.3±2
Ot	Ottawa	93°	3 ±2
W	Wingst	137°	0.8±2
Cf	Chambon la Forrét	142°	− 0.2±0.2
Ta	Tamanrasset	169°	< 4

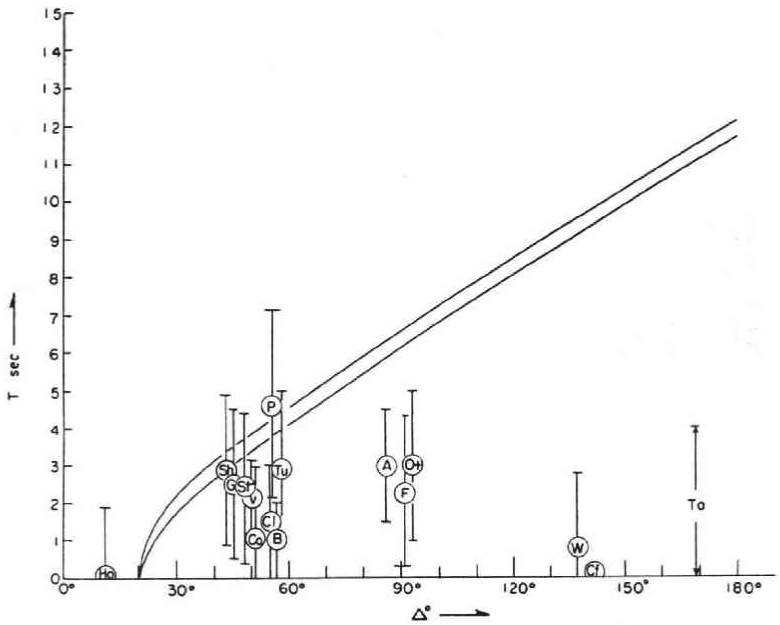

Fig. 5. Observed data with calculated theoretical curve in the case that the spread angle of source is 20°, h_0, the base of the magnetosphere, is 500 km (lower) and 400 km (upper)

Acknowledgement

We would like to express our hearty thanks to the directors of the magnetic observatories in the world who kindly sent us useful copies of the magnetograms.

Thanks due to Dr. B. CANER of the Victoria Magnetic Observatory, and Prof. E. SELZER and Prof. W.E. MCNICOL of the University of Qeensland for their interesting discussions.

The authors express their sincere thanks to Captain ROBERT A. EARLE of the U. S. Depertment of Commerce, Coast and Geodetic Survey for the valuable copies of rapid-run magnetogram in the United States.

References

B. CANER and K. WHITHAM: A Geomagnetic Observation of a High-altitude Nuclear Detonation. private communication but will be published in Canadian Journal of Physics.

J. ROQUET, R. SCHLICH and E. SELZER: Reception quasi-simultance en France, a Kerguelen et en Terre Adélie de la perturbation du champ magnétique terrestre engendrée par l'explosion nucleaire spatiale du 9 Juillet 1962. Académie des Sciences, Séance du 13 Aout 1962.

R.W.E. McNICOL and J.S. MAINSTONE: Geomagnetic Effects of Johnston Island High Altitude Thermo-Nuclear Explosion of 9th, July, 1962 (private communication).

B.J. FRASER: Geomagnetic Micropulsations from the High-Altitude Nuclear Explosion above Johnston Island. *Journal of Geophysical Research*, Vol. **67**, 4926, 1962

R.C. BAKER and W.M. STROME: Magnetic Distrubance from a High-Altitude Nuclear Explosion. *Journal of Geophysical Research*, Vol. **67**, 4927, 1962.

R.R. UNTERBERGER and P. EDWARD BYERLY: Magnetic Effects of a High-Altitude Nuclear Explosion. *Journal of Geophysical Research*, Vol. **67**, 4929, 1962.

EDWARD V. ASHBURN, JAMES P. LEE, and RAY N. FRANCIS: Observations of the Changes in the Earth's Magnetic Field Induced by the High-Altitude Nuclear Explosion of July 9, 1962. *Journal of Geophysical Research*, Vol. **67**, 4933, 1962.

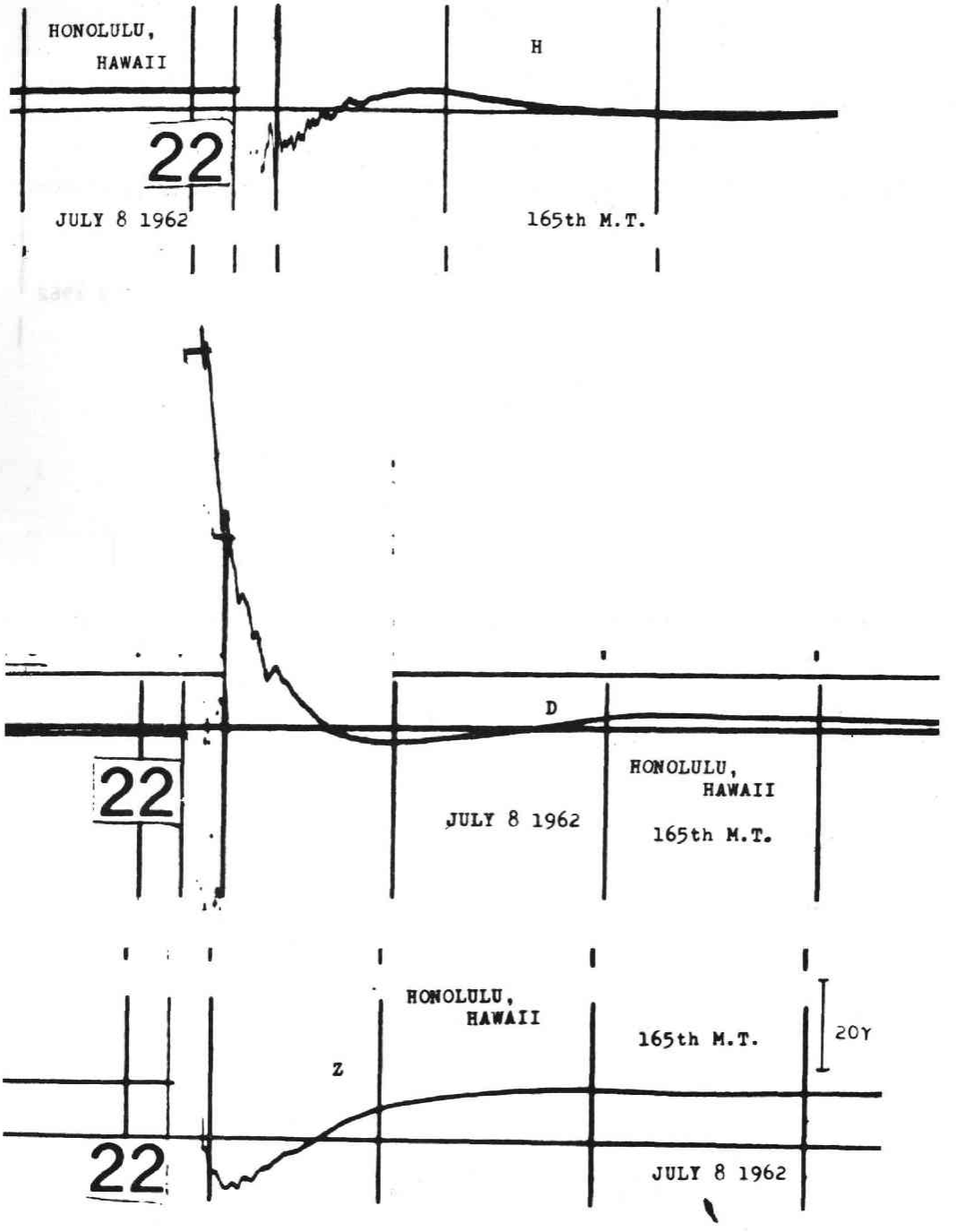
HONOLULU,
HAWAII
H
22
JULY 8 1962
165th M.T.
D
22
HONOLULU,
HAWAII
JULY 8 1962
165th M.T.
HONOLULU,
HAWAII
165th M.T.
20γ
Z
22
JULY 8 1962

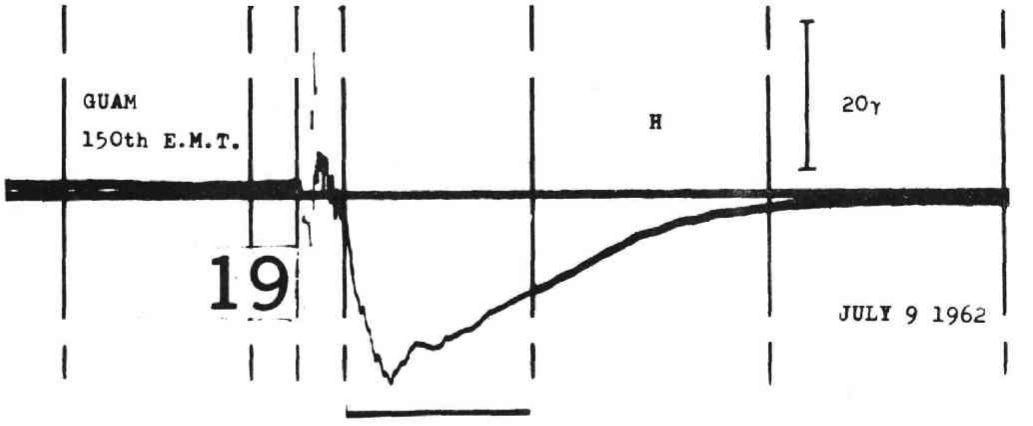
GUAM
150th E.M.T.
H
20γ
19
JULY 9 1962

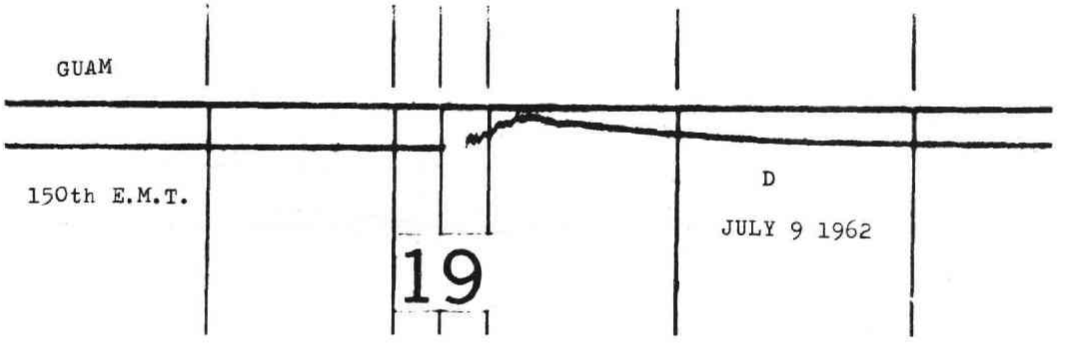
GUAM
150th E.M.T.
D
JULY 9 1962
19

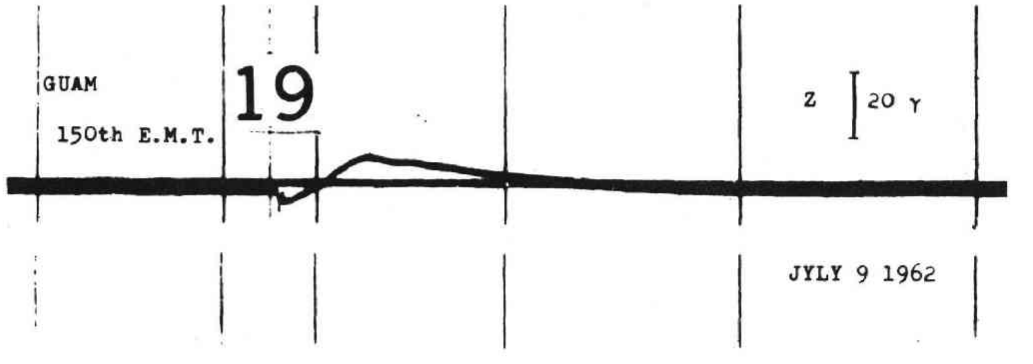
GUAM
150th E.M.T.
19
Z
20 γ
JYLY 9 1962

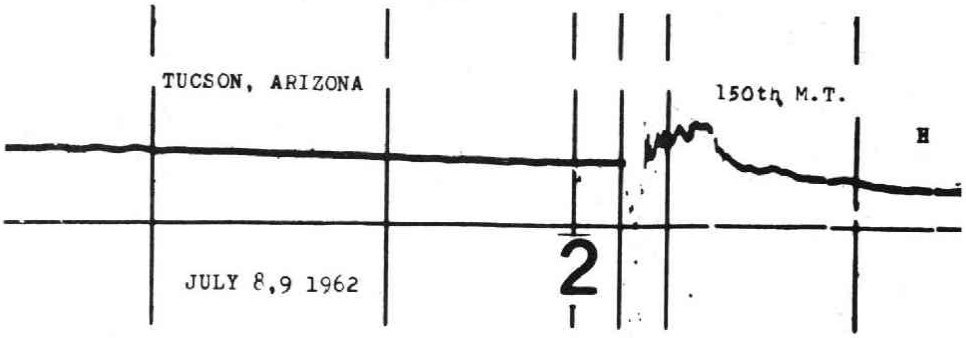
TUCSON, ARIZONA
150th M.T.
H
JULY 8,9 1962
2

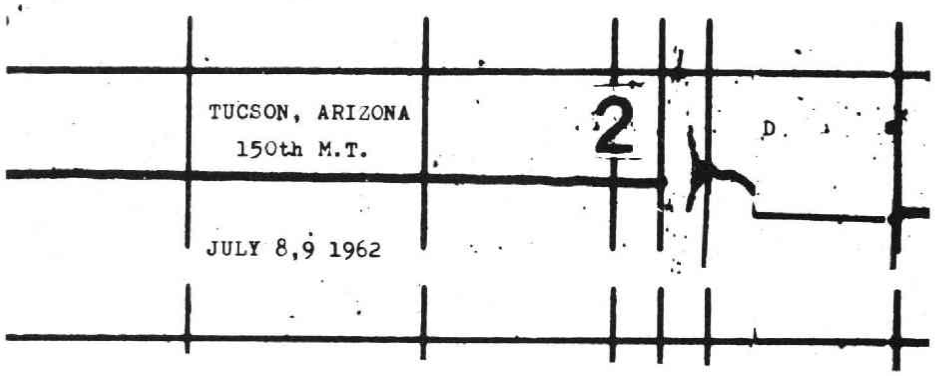
TUCSON, ARIZONA
150th M.T.
2
D
JULY 8,9 1962

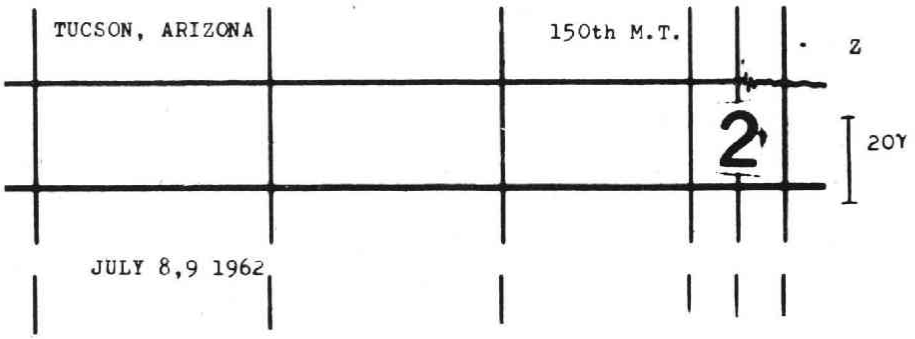
TUCSON, ARIZONA
150th M.T.
Z
2
20Y
JULY 8,9 1962

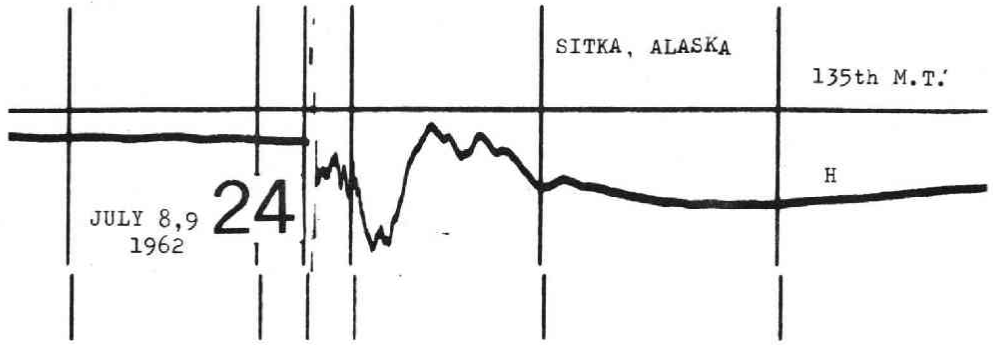
SITKA, ALASKA
135th M.T.
H
JULY 8,9
1962
24

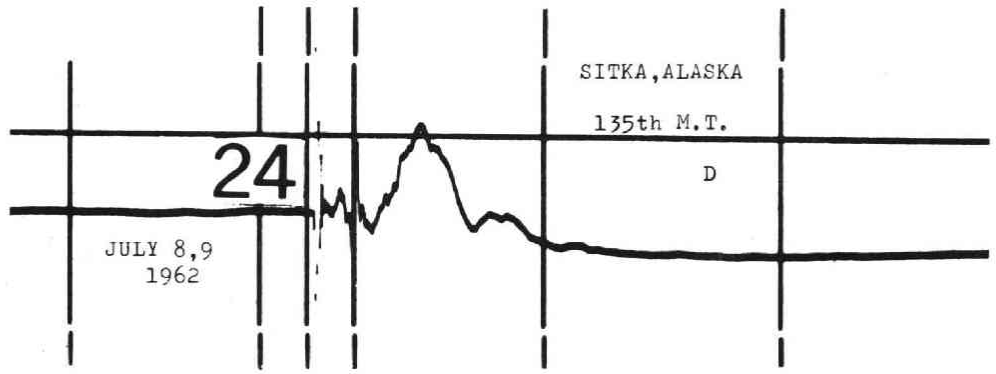
SITKA, ALASKA
135th M.T.
D
24
JULY 8,9
1962

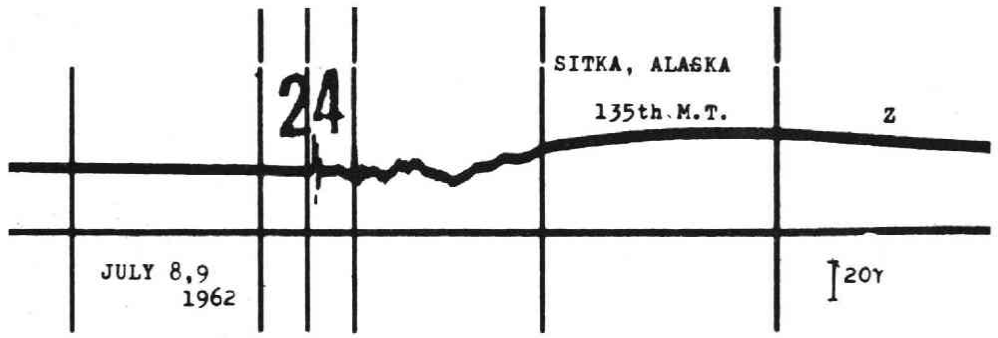
SITKA, ALASKA
135th M.T.
Z
24
JULY 8,9
1962
20γ

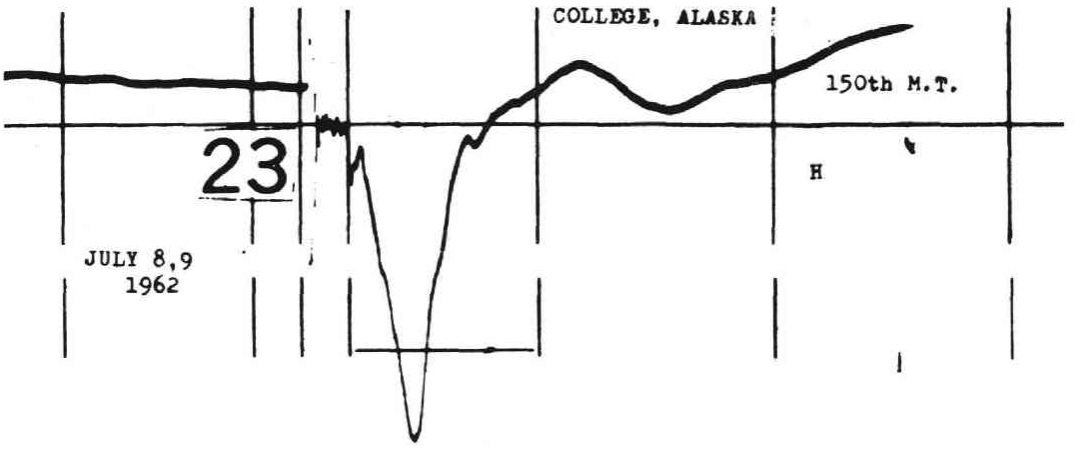
COLLEGE, ALASKA
150th M.T.
23
H
JULY 8,9
1962

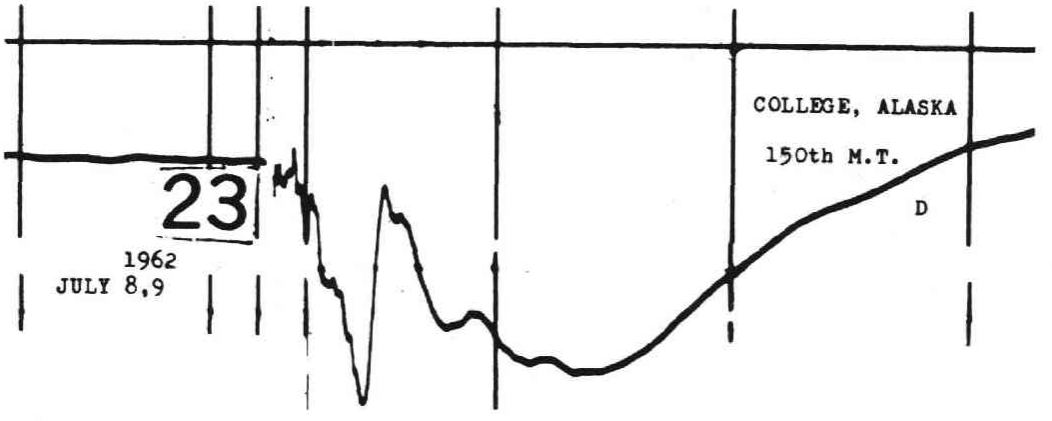
COLLEGE, ALASKA
150th M.T.
23
D
1962
JULY 8,9

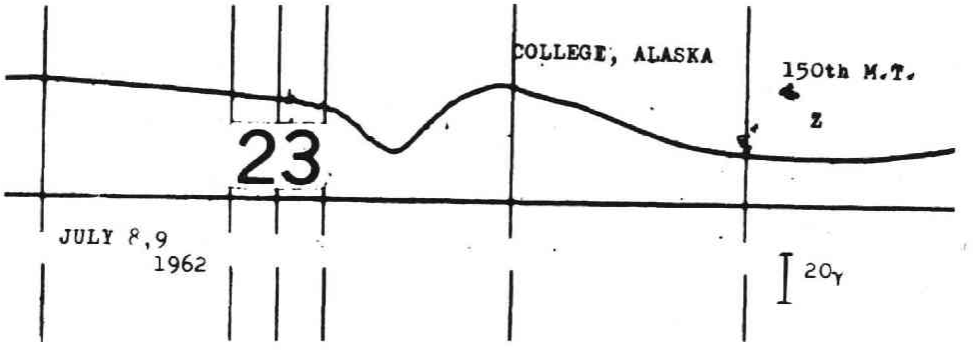
COLLEGE, ALASKA
150th M.T.
Z
23
JULY 8,9
1962
20γ

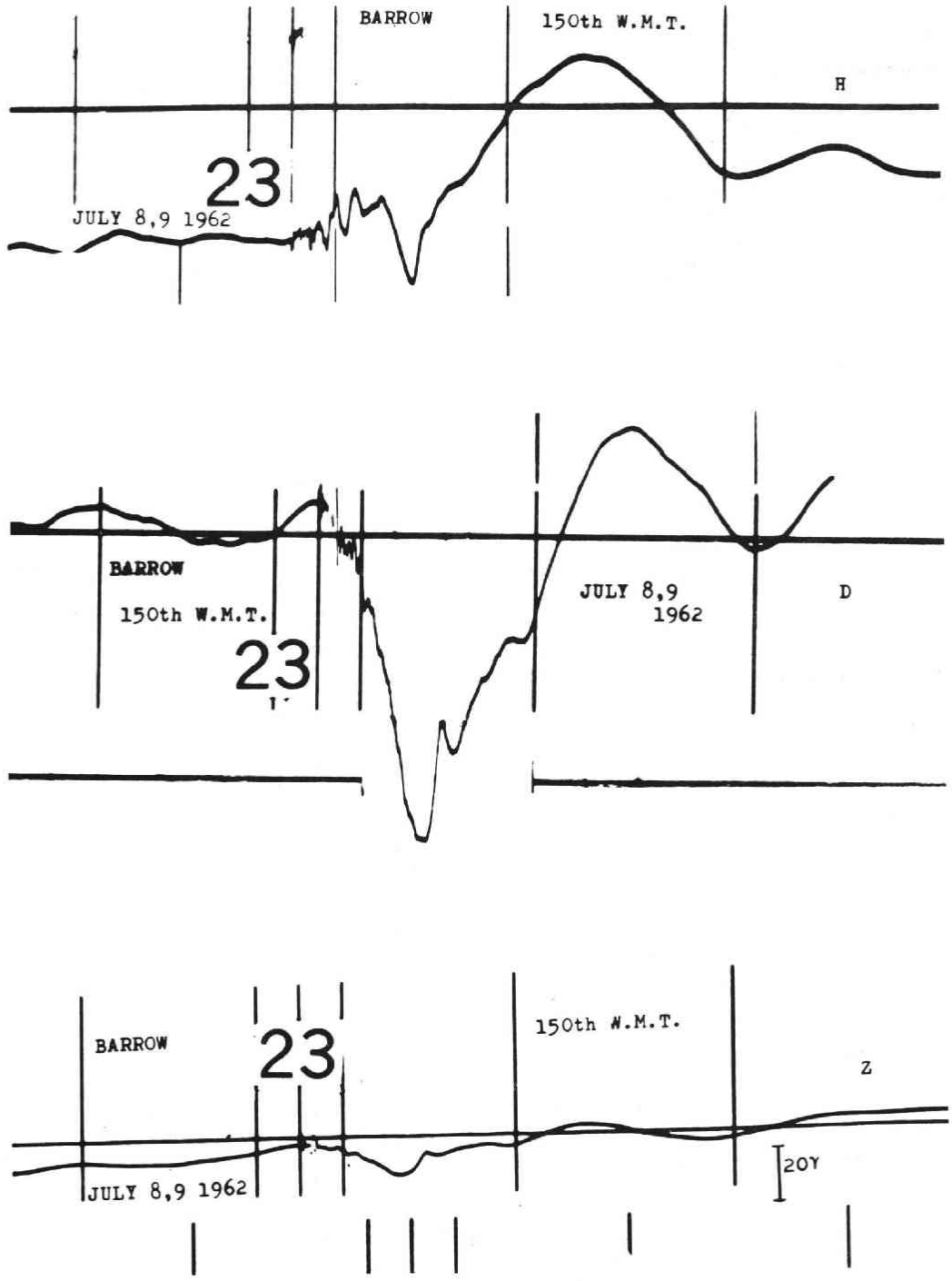
BARROW
150th W.M.T.
H
23
JULY 8,9 1962
BARROW
150th W.M.T.
23
JULY 8,9
1962
D
BARROW
23
150th W.M.T.
Z
20γ
JULY 8,9 1962

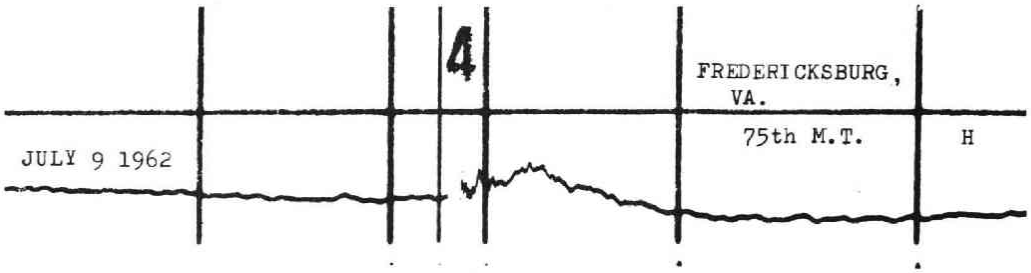
4
FREDERICKSBURG, VA.
75th M.T.
H
JULY 9 1962

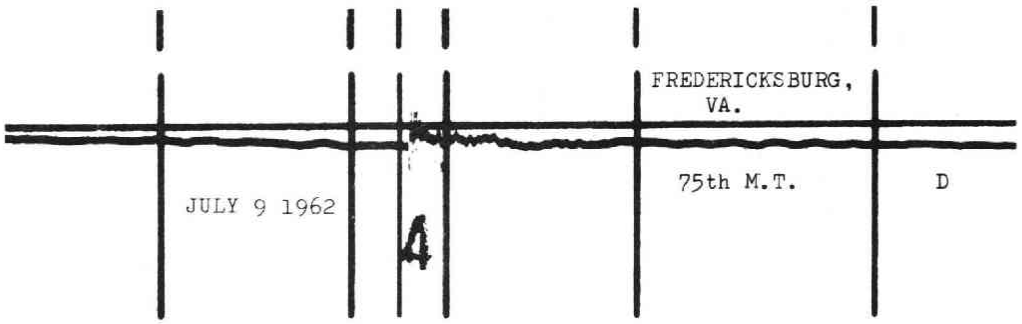
FREDERICKSBURG, VA.
75th M.T.
D
JULY 9 1962
4

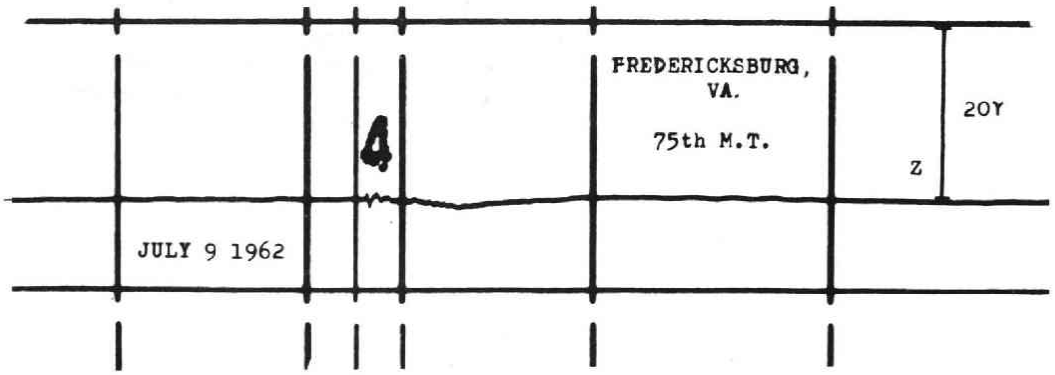
FREDERICKSBURG, VA.
75th M.T.
Z
20Y
4
JULY 9 1962

Amberley

July 9 1962

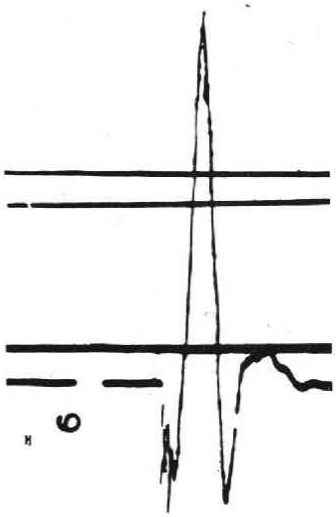

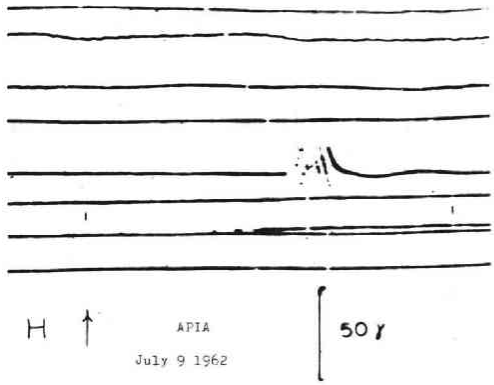

Amberley

July 9 1962

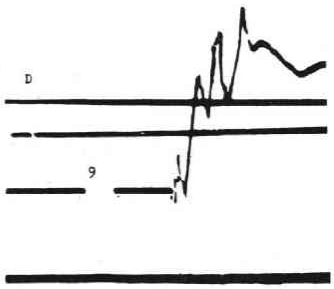

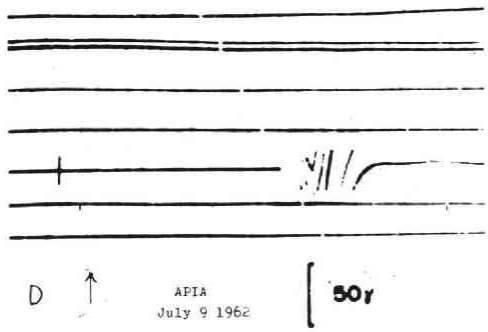

Amberley

July 9 1962

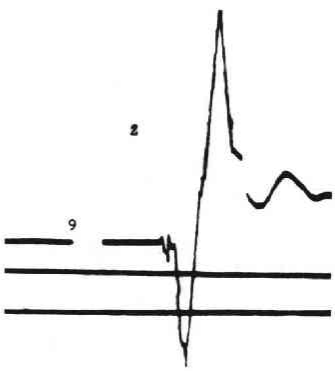

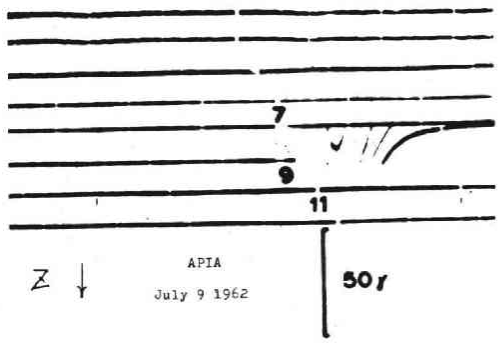

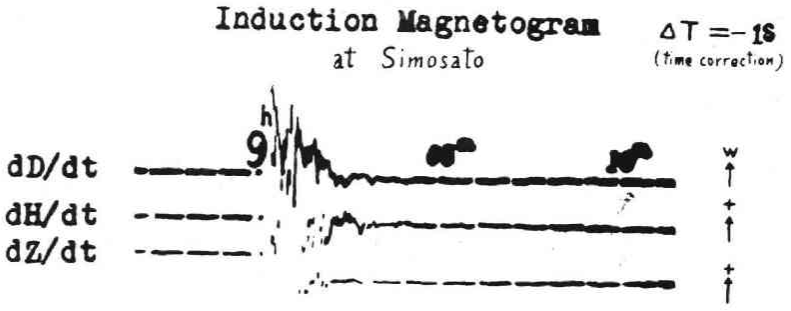
Induction Magnetogram
at Simosato
ΔT = −1S
(time correction)
dD/dt
dH/dt
dZ/dt
9h
W

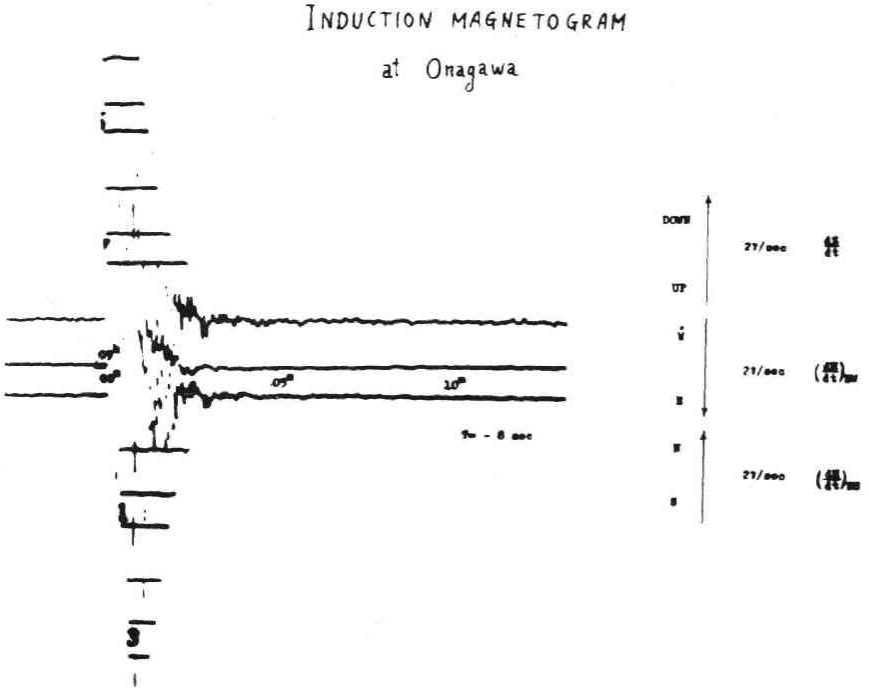
INDUCTION MAGNETOGRAM
at Onagawa
DOWN
UP
27/sec
27/sec
27/sec

BRISBANE July 9 1962

Tracks I, II and III representing pulsation in the frequency range 0.01, to 0.1 c/s in E-W vertical and N-S components.
Tracks IV records pulsations in N-S component in the frequency range 0.1~1 - 2 c/s

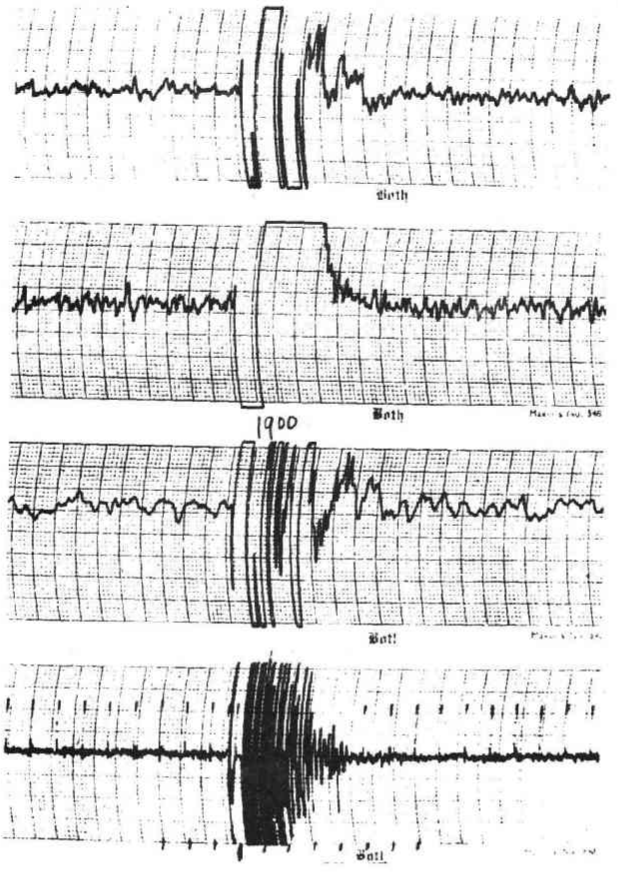

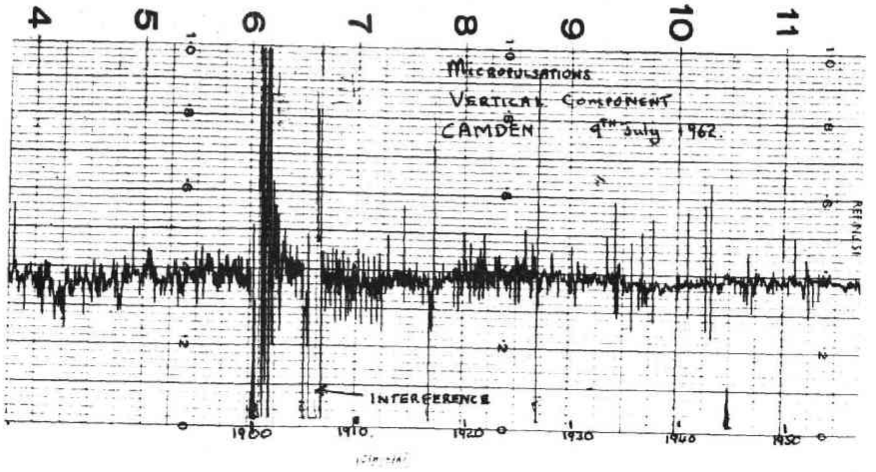

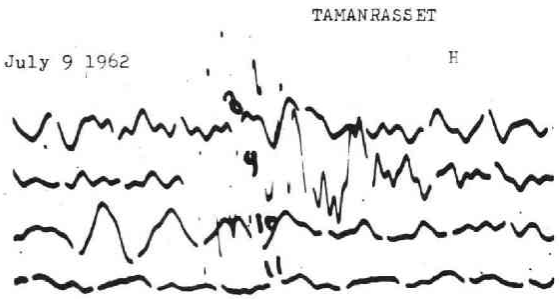
TAMANRASSET
July 9 1962
H

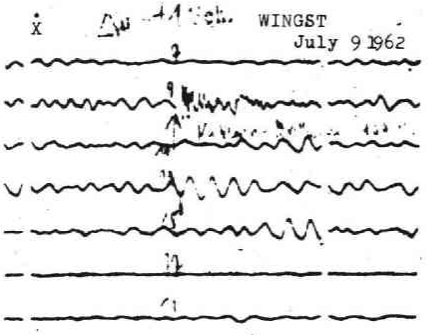
WINGST
July 9 1962
Ẋ

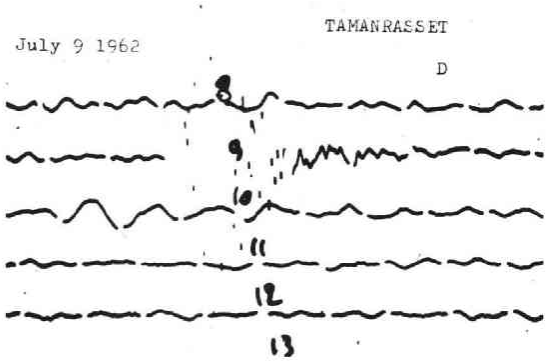
TAMANRASSET
July 9 1962
D

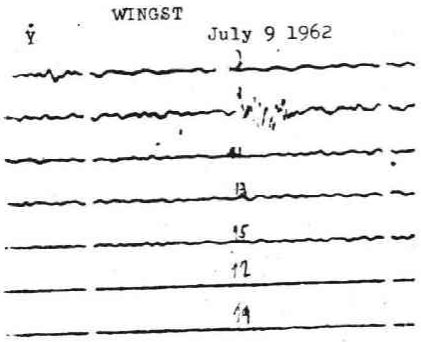
WINGST
July 9 1962
Ẏ

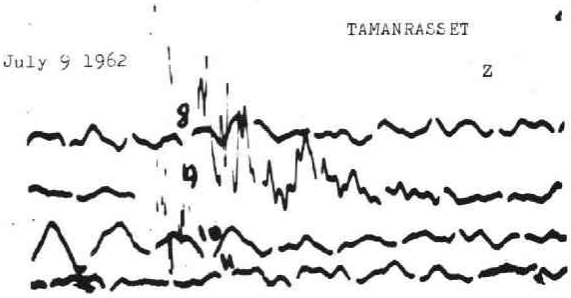
TAMANRASSET
July 9 1962
Z

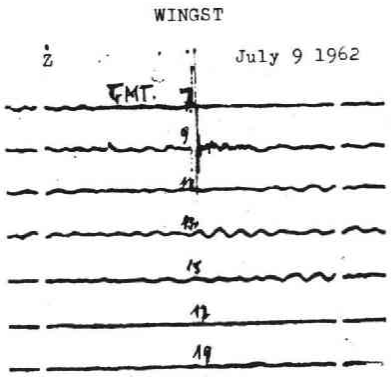
WINGST
July 9 1962
Ż
GMT.

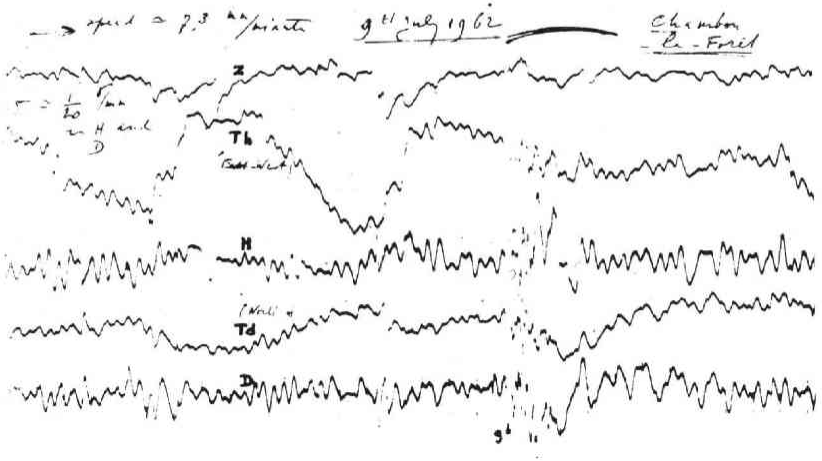
Z
Th
H
Td
D

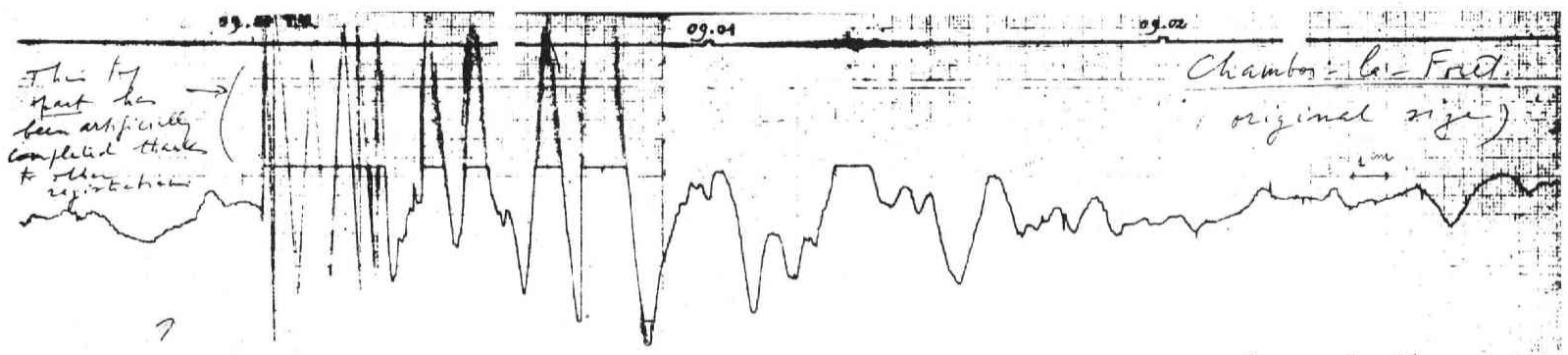
09.01
09.02
Chambon-la-Frêt
original size
1 mn
This trace has been artificially completed thanks to other registrations
This registration was specially designed to assure precise timing of the front of the signal.
Telluric registration South - North.
CHAMBON LA FORET July 9 1962

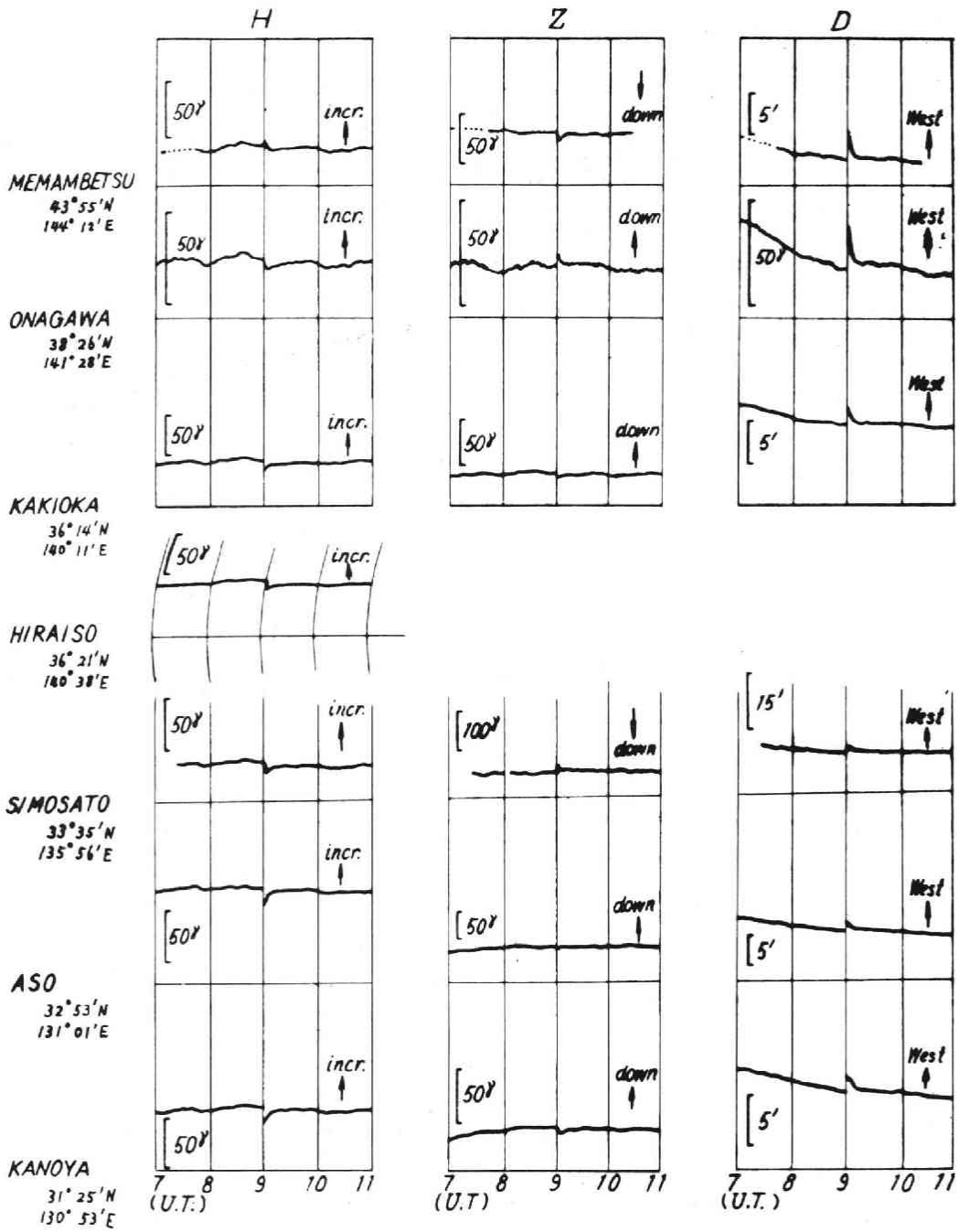
H
Z
D
MEMAMBETSU
43°55'N
144°12'E
ONAGAWA
38°26'N
141°28'E
KAKIOKA
36°14'N
140°11'E
HIRAISO
36°21'N
140°38'E
SIMOSATO
33°35'N
135°56'E
ASO
32°53'N
131°01'E
KANOYA
31°25'N
130°53'E
50γ
incr.
down
5'
West
100γ
15'
7
8
9
10
11
(U.T.)

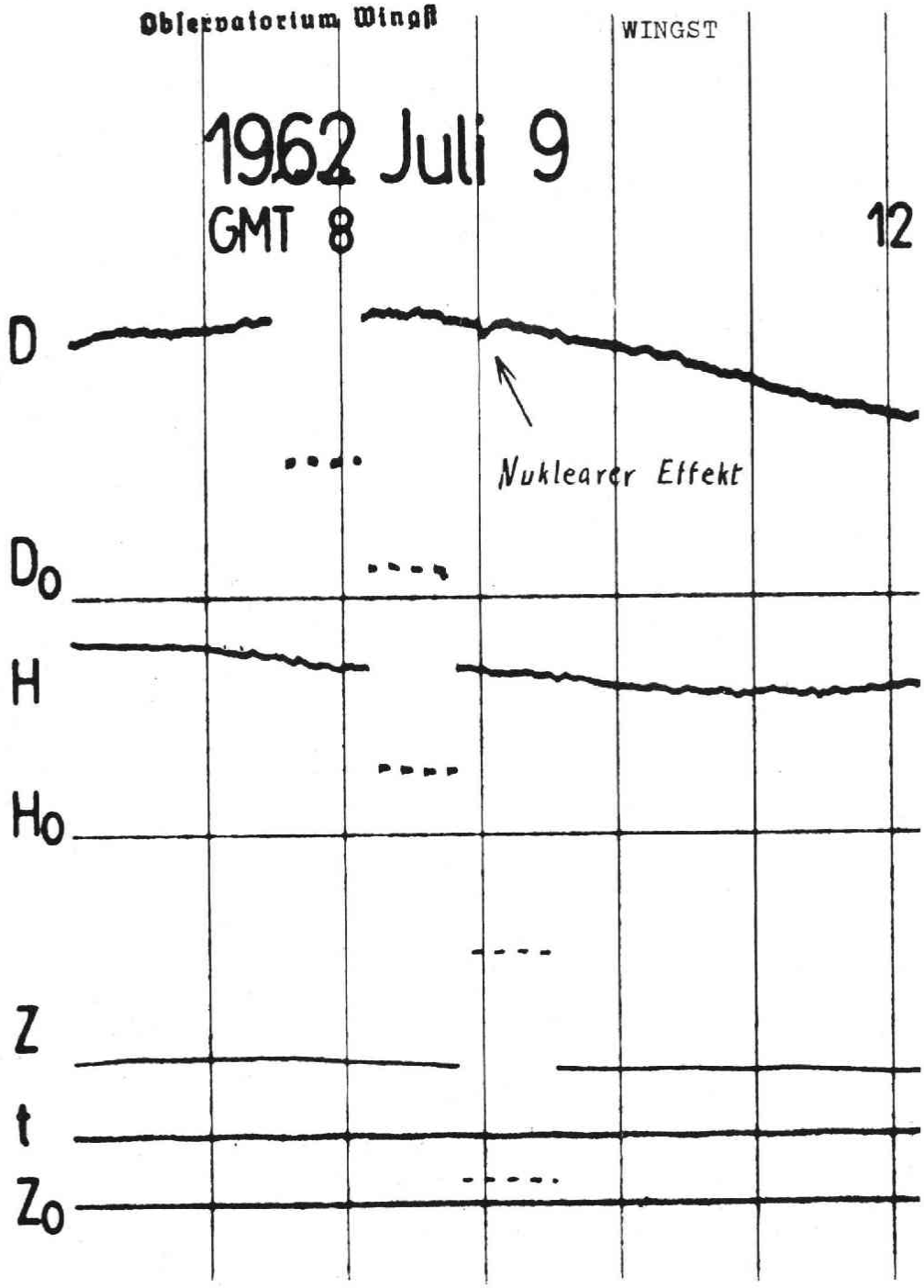
Observatorium Wingst
WINGST
1962 Juli 9
GMT 8
12
D
Nuklearer Effekt
Do
H
Ho
Z
t
Zo

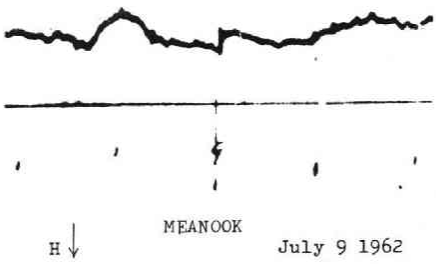
MEANOOK
H
July 9 1962

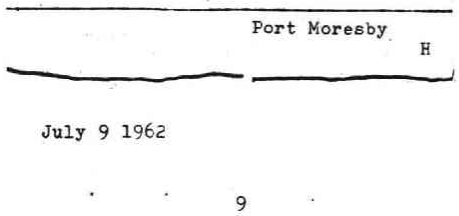
Port Moresby
H
July 9 1962
9

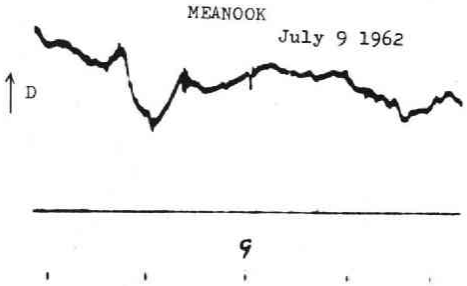
MEANOOK
July 9 1962
D
9

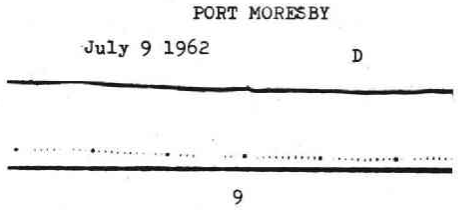
PORT MORESBY
July 9 1962
D
9

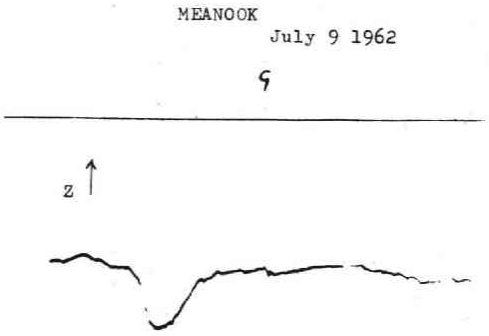
MEANOOK
July 9 1962
9
Z

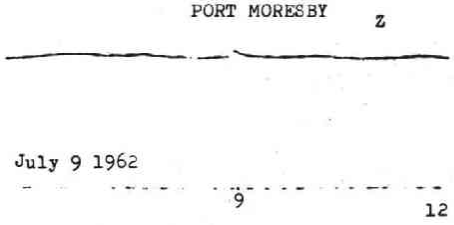
PORT MORESBY
Z
July 9 1962
9
12

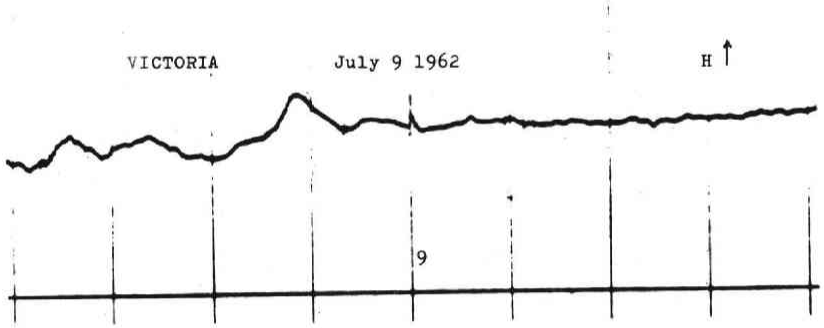
VICTORIA
July 9 1962
H
9

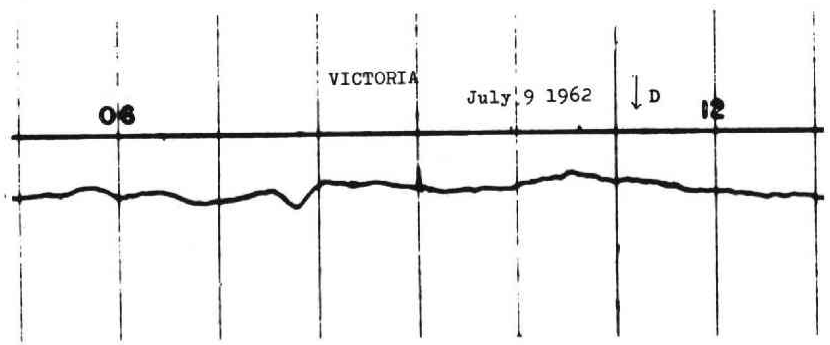
06
VICTORIA
July 9 1962
D
12

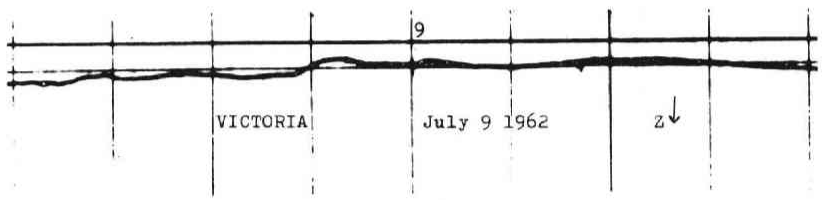
9
VICTORIA
July 9 1962
Z

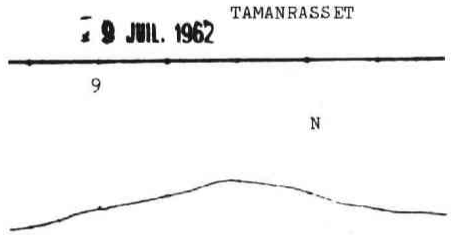
9 JUIL. 1962
TAMANRASSET
9
N

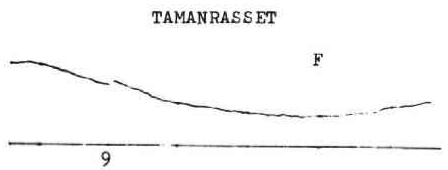
TAMANRASSET
F
9

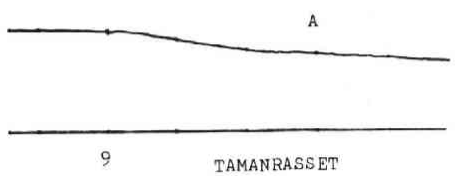
A
9
TAMANRASSET

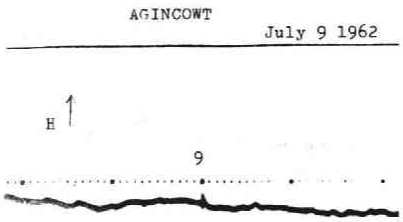
AGINCOWT
July 9 1962
H
9

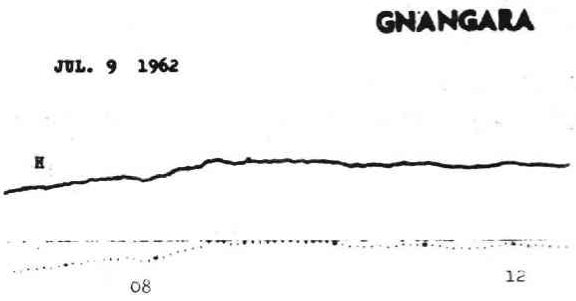
GNANGARA
JUL. 9 1962
H
08
12

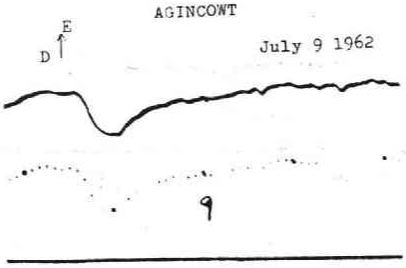
AGINCOWT
July 9 1962
D
E
9

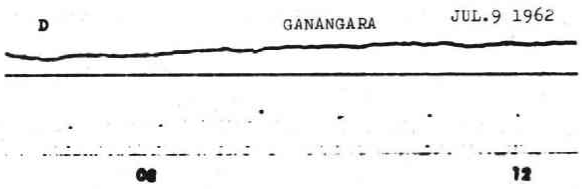
D
GANANGARA
JUL.9 1962
08
12

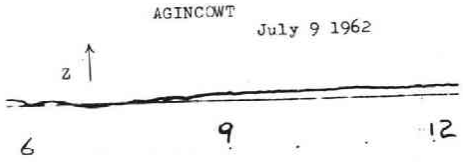
AGINCOWT
July 9 1962
Z
6
9
12

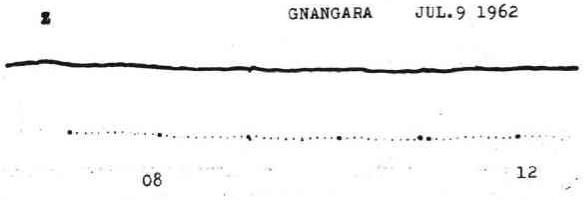
Z
GNANGARA
JUL.9 1962
08
12

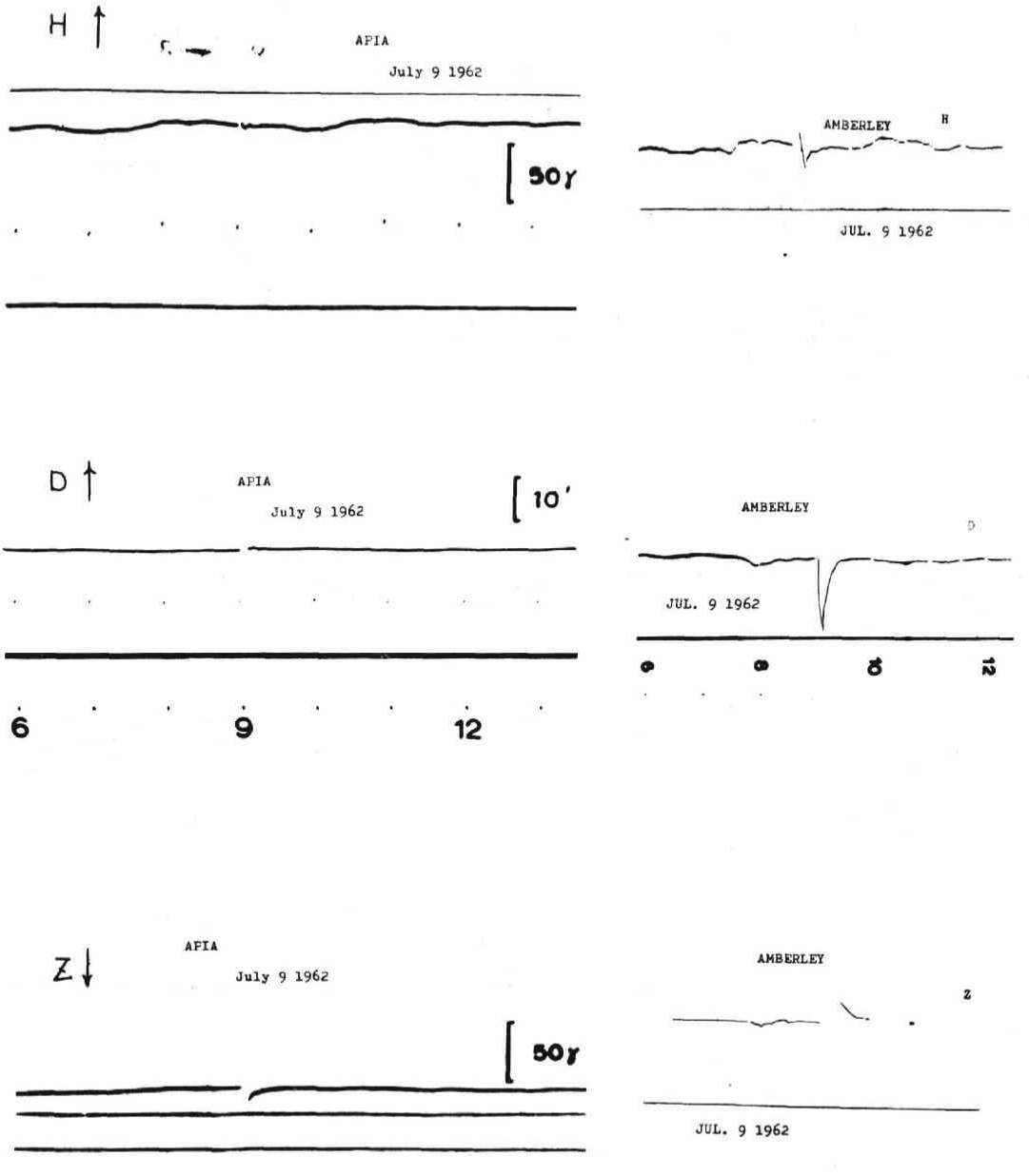
H
APIA
July 9 1962
50γ
AMBERLEY
H
JUL. 9 1962
D
APIA
July 9 1962
10'
AMBERLEY
D
JUL. 9 1962
6
9
12
Z
APIA
July 9 1962
50γ
AMBERLEY
Z
JUL. 9 1962